

CYP6B1 and CYP6B3 of the Black Swallowtail (*Papilio polyxenes*): Adaptive Evolution through Subfunctionalization

Zhimou Wen,* Sanjeewa Rupasinghe,* Guodong Niu,† May R. Berenbaum,† and Mary A. Schuler*

*Department of Cell and Developmental Biology, University of Illinois; and †Department of Entomology, University of Illinois

Gene duplication provides essential material for functional divergence of proteins and hence allows organisms to adapt to changing environments. Following duplication events, redundant paralogs may undergo different evolutionary paths via processes known as nonfunctionalization, neofunctionalization, or subfunctionalization. Studies of adaptive evolution at the molecular level have progressed rapidly by computationally analyzing nucleotide substitution patterns but such studies are limited by the absence of information relating to alterations of function of the encoded enzymes. In this respect, evolution of the *Papilio polyxenes* cytochrome P450 monooxygenases (P450s) responsible for the adaptation of this insect to furanocoumarin-containing host plants provides an excellent model for elucidating the evolutionary fate of duplicated genes. Evidence from sequence and functional analysis in combination with molecular modeling indicates that the paralogous *CYP6B1* and *CYP6B3* genes in *P. polyxenes* have probably evolved via subfunctionalization after the duplication event by which they arose. Both enzymes have been under independent purifying selection as evidenced by the low dN/dS ratio in both the coding region and substrate recognition sites. Both enzymes have maintained their ability to metabolize linear and angular furanocoumarins albeit at different efficiencies. Comparisons of molecular models developed for the *CYP6B3* and *CYP6B1* proteins highlight differences in their binding modes that account for their different activities toward linear and angular furanocoumarins. That *P. polyxenes* maintains these 2 furanocoumarin-metabolizing loci with somewhat different activities and expression patterns provides this species with the potential to acquire P450s with novel functions while maintaining those most critical to its exclusive feeding on its current range of host plants.

Introduction

Gene duplication provides essential material for functional divergence of proteins and hence allows organisms to adapt to changing environments. Following duplication events, redundant paralogs resulting from gene duplication events may undergo different evolutionary paths. The most common process is known as nonfunctionalization where one copy, under purifying selection, maintains the ancestral function whereas the other copy is free to accumulate loss-of-function mutations. Though rare, however, viable mutations in the coding or regulatory regions of the duplicated copy do occasionally have the potential to create new advantageous functions in a process known as neofunctionalization. The original function may also partition among paralogs via a process known as subfunctionalization (Prince and Pickett 2002; Long et al. 2003; Meyer and Van de Peer 2003; Zhang 2003). Although computational analysis of nucleotide substitution patterns have provided insight into adaptive evolution occurring at the level of DNA and protein sequences, these studies are plagued by the absence of information on the process of functional evolution in enzymes in response to environmental selection pressures (Hughes 2002). In this respect, the cytochrome P450 monooxygenases (P450s) contributing to the adaptation of *Papilio polyxenes* to furanocoumarin-containing host plants are excellent models for analyzing constraints on functional evolution.

P450s, a superfamily of enzymes that metabolizes a wide variety of endogenous and exogenous compounds, originated from an extensive series of gene duplications with subsequent adaptive diversification resulting from

antagonistic interactions between animals and plants in the ensuing years (Gonzalez and Nebert 1990; Feyereisen 2005). The stepwise coevolution between furanocoumarin-containing plants and insects that feed exclusively on these toxin-laden plants exemplifies the role of P450s in insect-plant interactions (Schuler 1996; Berenbaum 2002).

Furanocoumarins, found in several plant families including Apiaceae and Rutaceae, are toxic to many organisms due to their ability to crosslink DNA and inactivate proteins in the presence of ultraviolet light (Berenbaum 1991). Despite their toxicity, some specialist insects, including the majority of species in the lepidopteran genus *Papilio*, feed exclusively on host plants containing furanocoumarins; such oligophagy is facilitated by the ability to rapidly and efficiently detoxify these toxins via P450-mediated systems (Ivie et al. 1983, 1987; Bull et al. 1986; Schuler 1996; Berenbaum 2002; Li et al. 2003; Mao et al. 2006).

Cloning and characterization of P450 genes in the CYP6B subfamily from *Papilio* species, ranging from generalists that rarely encounter furanocoumarins to specialists that feed exclusively on furanocoumarin-containing host plants, have led to a better understanding of the evolution of insect-host plant specialization. Commonalities in the protein sequences, intron/exon arrangements, and xanthotoxin- and xenobiotic-responsive promoter elements suggest that *CYP6B* loci have a common ancestral origin (Cohen et al. 1992; Prapaipong et al. 1994; Hung et al. 1996, 1997; Li et al. 2001, 2002; Petersen et al. 2001; McDonnell et al. 2004). This phylogenetic association and subsequent divergence of *Papilio* CYP6B members is further substantiated by the varying furanocoumarin-metabolic activities of different CYP6B proteins across species. The metabolic efficiencies of these different P450s range from the low activities for CYP6B4- and CYP6B17-group members from *Papilio canadensis* (a generalist feeding rarely, if ever, on furanocoumarin-containing plants), to intermediate activities for CYP6B4- and CYP6B17-group members from *Papilio glaucus* (a generalist feeding occasionally on furanocoumarin-containing plants),

Key words: adaptive evolution, subfunctionalization, cytochrome P450 monooxygenases (P450s), molecular modeling of detoxification enzymes, plant-insect interactions.

E-mail: maryschu@uiuc.edu.

Mol. Biol. Evol. 23(12):2434–2443. 2006

doi:10.1093/molbev/msl118

Advance Access publication September 19, 2006

to very high activities for CYP6B1 from *P. polyxenes* (a specialist feeding exclusively on furanocoumarin-containing plants) (Chen et al. 2002; Baudry et al. 2003; Li et al. 2003; Wen et al. 2003). Phylogenetic and substrate recognition site (SRS) analysis of contemporary papilionid CYP6B proteins coupled with estimates of metabolic activities indicate that host plant diversity is related directly to the diversity of P450 activities in an insect and inversely related to substrate specificity of individual enzymes. As examples, by virtue of continual exposure to furanocoumarins in its host plants, CYP6B1 in *P. polyxenes* is hypothesized to have evolved from an ancestral protein in a polyphagous ancestor having low activities toward a broad range of substrates into a highly specialized P450 having high activity toward a narrow range of linear and angular furanocoumarins (Li et al. 2003).

Subsequent to the acquisition of CYP6B1-type proteins in *Papilio* species facilitating exclusive use of furanocoumarin-containing plants, maintenance of the integrity of these enzymes is essential for continued utilization of these toxic host plants. Any compromise in the expression of fully functional CYP6B1-group proteins in these insects might be expected to be selected against. Given that even conservative changes of single amino acids (e.g., isoleucine to leucine) in CYP6B1 dramatically compromise this enzyme's furanocoumarin metabolic capacities (Chen et al. 2002; Pan et al. 2004; Wen et al. 2005), the integrity of CYP6B1 and any other furanocoumarin-metabolizing P450s is essential even as new metabolic activities evolve.

Of the 2 paralogous P450s originally cloned from *P. polyxenes*, CYP6B1 (Cohen et al. 1992) and CYP6B3 (Hung et al. 1995), CYP6B1 has few metabolic capabilities beyond the metabolism of furanocoumarins typically found in swallowtail host plants (Chen et al. 2002; Wen et al. 2003, 2005; Pan et al. 2004). Among the 3 cloned CYP6B1 allelic variants (Cohen et al. 1992; Prapaipong et al. 1994), CYP6B1v1 and CYP6B1v2 metabolize furanocoumarins with similar capacities (Ma et al. 1994) and CYP6B1v3 is so closely related to these proteins (99.4% amino acid identity with CYP6B1v1) that it is expected to have similar activities. The 2 allelic CYP6B3 variants identified by Hung et al. (1995, 1996) share approximately 88% amino acid identity with CYP6B1 proteins. To explore the genetic basis for variation in furanocoumarin metabolism in *P. polyxenes*, we cloned 5 additional variants of CYP6B3. Comparative analyses of these with CYP6B1 sequences at both the nucleotide and amino acid levels suggest that these paralogous genes have evolved by subfunctionalization after their original duplication. To gain further insight into the evolution of these 2 paralogs, we have heterologously expressed 2 of the CYP6B3 variants and CYP6B1v1 in Sf9 insect cells along with cytochrome P450 reductase. These studies indicate that the CYP6B3 variants also metabolize both linear and angular furanocoumarins but at lower efficiency and in different rank order than CYP6B1. Molecular modeling of the catalytic sites in these 2 groups of P450s highlights regions of the catalytic site where amino acid replacements account for the lower metabolic activities of CYP6B3 toward furanocoumarins.

Materials and Methods

Chemicals

Xanthotoxin (8-methoxypsoralen), bergapten (5-methoxypsoralen), trioxsalen, isopimpinellin, psoralen, and angelicin were purchased from Indofine Chemical (Belle Mead, NJ); sphondin was from Dr Arthur Zangerl (University of Illinois at Urbana-Champaign [UIUC]); visnagin, khellin, flavone, and α -naphthoflavone were bought from Aldrich Chemical (Milwaukee, WI); coumarin, β -nicotinamide adenine dinucleotide phosphate (NADPH), cytochrome c, heat-inactivated fetal bovine serum and hemin were obtained from Sigma Chemical (St Louis, MO). Reagents for heterologous expression in Sf9 insect cells were purchased from GibcoBRL/Life Technology (Grand Island, NY). Xanthotoxin labeled with [14 C] on the methoxy carbon was kindly provided by Dr Wenfu Mao (UIUC).

Cloning and Sequencing the Coding Region of CYP6B3 Allelic Variants

Total RNA was isolated from midguts of 3-day-old fifth instar larvae of *P. polyxenes* using TRIzol reagents (Invitrogen, Carlsbad, CA) following the manufacturer's instructions. Five micrograms of total RNA were then used for first strand cDNA synthesis by Superscript III (Invitrogen) using an oligo(dT)₁₇ primer (5'-CGGAATTCCTTTTT-TTTTTTTTTT-3'). CYP6B3 coding sequences (CDSs) were PCR amplified using first strand cDNA and the GZF1/GZR1 primer set designed to amplify the CYP6B3v1 cDNA sequence (GenBank accession number U25819). The GZF1 forward primer (5'-ATGTTGATGTTATAACTCTTGTTACGG-3') contains the CYP6B3 start codon (underlined) and the GZR1 reverse primer (5'-ctgcagTTATCTGCGGACAATGTTTAC-3') contains the CYP6B3 stop codon (underlined) and a terminal *Pst* I restriction site (lower case). Platinum *Pfx* (Invitrogen) was used in PCR reactions that were heated at 94°C for 5 min, followed by 30 cycles of amplification (1 min for 94°C, 1 min for 55°C, and 2 min for 72°C) and finished with a final extension at 72°C for 10 min. The 1.5 kb PCR product was cloned directly into the pGEM-T easy vector (Promega, Madison, WI) and positive clones were identified by colony PCR using the GZF1/GZR1 primer set. Because GZF1/GZR1 amplifies both CYP6B1 and CYP6B3, another round of stringent colony PCR was performed to screen for CYP6B3 clones using the GZF2/GZR2 primer set specific for CYP6B3 (GZF2 forward primer 5'-CCATCTTCCCGAAGGTTGTTAAA-3'; GZR2 reverse primer 5'-GCCCTTCTTGATAGTGATGTCA-3') to generate a 495 bp CYP6B3-specific product. Inserts of 30 clones positive for the GZF2/GZR2 primer set and 3 clones positive for the GZF1/GZR1 primer set but negative for the GZF2/GZR2 primer set were sequenced in their entirety using vector and internal primers.

Sequence Analyses

Amino acid sequences were first aligned using the ClustalW function built in the MEGA program (version 3.1, Kumar et al. 2004) and their coding nucleotides were then aligned using the amino acid alignment as a phasing

guide (i.e., gaps were inserted in-frame to maintain the reading frame). Single nucleotide polymorphisms (SNPs) were identified as synonymous (S) and nonsynonymous (NS) substitutions. Amino acid substitutions were defined as highly conservative, weakly conservative, or nonconservative based on ClustalW functions in Biology Workbench (<http://workbench.sdsc.edu>). The values of p-distance (number of nucleotide substitutions per site) for each pair of sequences were calculated and average values obtained for both collections of CYP6B1 and CYP6B3 variants. The values of p-distance, dS (number of nucleotide substitutions per synonymous site), and dN (number of nucleotide substitutions per nonsynonymous site) were estimated using the Nei-Gojobori method with multiple substitutions at the same site corrected by Jukes-Cantor method implemented in the MEGA program. For the estimation of dS and dN values, the modified Nei-Gojobori (Jukes-Cantor) method was used with the transition/transversion ratio set at 2. Unrooted phylogenetic trees were constructed using different methods built in the MEGA program and the inferred phylogeny was tested by bootstrap analysis with 500 replications.

Coexpression of CYP6B1 and CYP6B3 Variants with Cytochrome P450 Reductase

CYP6B3 recombinant baculovirus constructions and coexpression in Sf9 cells with housefly P450 reductase were carried out as described for CYP6B1 in Wen et al. (2003) and Pan et al. (2004). Briefly, CYP6B3 proteins were coexpressed with housefly P450 reductase in Sf9 cells at a multiplicity of infection (MOI) of 2:2 (P450:P450 reductase). Hemin was supplemented to a final concentration of 5 µg/ml at the time of infection. Baculovirus-infected cells were harvested 72 h postinfection by centrifugation at 3000 × g for 10 min, washed once with one-half cell culture volume of 100 mM sodium phosphate buffer (pH 7.8) and once with one-tenth cell culture volume of cell lysate buffer (100 mM sodium phosphate [pH 7.8], 1.1 mM ethylenediaminetetraacetic acid, 0.1 mM dithiothreitol, 0.5 mM phenylmethylsulfonyl fluoride, 5 µg/ml [w/v] leupeptin, 20% glycerol). Cells were resuspended in one-tenth cell culture volume of cell lysate buffer, sonicated 2 times for 30 s in 5 ml batches on ice, vortexed for 15 s and centrifuged at 3000 × g for 10 min. Cell lysates (i.e., supernatants) were used immediately or aliquoted, frozen in liquid nitrogen, and stored at -80°C.

Metabolism Assays

CYP6B3 metabolism reactions were carried out exactly as described for CYP6B1 in previous reports (Wen et al. 2003, 2005). Briefly, 500 µl duplicate reactions were set up in 1 dram glass vials with each reaction containing final concentrations of 0.1 µM CYP6B1 or CYP6B3 proteins coexpressed with housefly P450 reductase (MOI ratio of 2:2), 0.3 mM NADPH and 100 µM (xanthotoxin, bergapten, and psoralen), 25 µM (angelicin and sphondin), or 10 µM (visnagin, khellin, flavone, coumarin, and α -naphthoflavone). Duplicate controls included reactions that were quenched at the beginning of each reaction with 125 µl 2 N HCl (zero-time control used for total substrate determinations) and reactions incubated in the absence of

NADPH (no NADPH control used for P450-independent activity determinations). Reactions were initiated with NADPH, incubated at 30°C for 20 min in a shaking water bath and terminated with the addition of 125 µl 2 N HCl. For internal standardization of extraction and injection efficiencies, the same amount of a second compound with a unique HPLC retention time was added; psoralen was used as internal control for xanthotoxin metabolism and xanthotoxin was used as control for the metabolism of all of the other compounds. Following addition of ethyl acetate to each reaction (2 ml to metabolism reactions of xanthotoxin, bergapten, and psoralen; 1 ml to metabolism reactions of angelicin and sphondin; 500 µl to metabolism reactions of all the other compounds), the samples were vortexed for 15 s and centrifuged at 2000 × g for 10 min. The upper ethyl acetate phase was directly analyzed on a normal phase high-pressure liquid chromatography column using a solvent mixture containing 80% cyclohexane, 18% ethyl ether, and 2% butanol. After correcting against the internal standard, the parent compound remaining in each sample was compared with parent compound present in the zero-time control following correction for P450-independent metabolism of each substrate. No P450-independent metabolism was detected for any of the compounds tested. Enzymatic activities were expressed as nmol substrate disappearance per min per nmol P450. Quantification of metabolism of each compound was replicated at least 3 times with cell lysates prepared from at least 3 independent batches of coexpressed proteins.

Metabolism of [¹⁴C] Xanthotoxin

CYP6B1 and CYP6B3 metabolism assays with [¹⁴C] methoxy-labeled xanthotoxin were carried out as described with single reactions of 500 µl set up in 1 dram glass vials (~4 ml, Fisher Scientific) containing final concentrations of 0.1 µM CYP6B1 or CYP6B3 protein coexpressed with housefly P450 reductase (MOI ratio of 2:2), 0.3 mM NADPH, 10 µM unlabeled xanthotoxin, and trace amounts of [¹⁴C] xanthotoxin (1 µl delivered in methanol). Reactions were initiated with NADPH, incubated for 30 min at 30°C and terminated with the addition of 125 µl 2 N HCl. To determine if CYP6B3 transforms the metabolites of xanthotoxin, 2 additional CYP6B1v1 reactions in the presence of NADPH were set up, incubated for 30 min at 30°C and subsequently supplemented with 0.1 µM CYP6B3v3 or CYP6B3v5, buffer and NADPH to a final total volume to 700 µl. These reactions were incubated for an additional 30 min and terminated with the addition of 175 µl 2 N HCl. A total of 24 µl reactions (or 33.6 µl for the reactions analyzing the combination of CYP6B1 and CYP6B3 variants) were spotted on a Silica Gel 60 F₂₅₄ precoated thin layer chromatography (TLC) plate (20 × 20 cm, 250 µm thick; Merck, Germany). Plates were developed using ethyl acetate:methanol:acetic acid (75:25:1) (Ivie et al. 1983), and radioactivity was detected by autoradiography and phosphorimager analysis.

Molecular Modeling and Substrate Docking

Models of these 3 insect P450s were developed using the two-class alignment procedures described in Baudry

et al. (2006) that distinguish between Class II P450s (those utilizing membrane-bound NADPH P450 reductase as an electron transfer partner) and Class I P450s (those utilizing soluble electron transfer partners). Using the alignment of each CYP6B protein with 8 Class II proteins, mammalian CYP3A4 (1TQN) (Yano et al. 2004), CYP2C8 (1PQ2) (Schoch et al. 2004), CYP2B4 (1SUO) (Scott et al. 2004), CYP2C5 (1N6B) (Wester et al. 2003), CYP2C9 (1OG5) (Williams et al. 2003), CYP2A6 (1Z11) (Yano et al. 2005), bacterial CYP102 (2HPD) (Ravichandran et al. 1993), and bacterial CYP175A1 (1N97) (Yano et al. 2003), models for CYP6B1, CYP6B3v3, and CYP6B3v5 were constructed using a hybrid template with most of the backbone coordinates obtained from CYP2A6 and backbone coordinates for the B-B' loop, B helix and B-C loop obtained from CYP2B4. In the MOE programs (Chemical Computing Group, Montreal, Canada) used for this analysis, 10 models for each target were generated and models were ranked according to the residue packing function provided in the MOE program.

Docking of prospective ligands was performed using LigandFit (Venkatachalam et al. 2003) implemented in the program Cerius2 (Version 4.10; Accelrys, San Diego, CA). LigandFit employs a cavity-detection algorithm combined with a fast ligand conformational search engine that allows the optimization of the bond structure of a ligand in a protein cavity, together with the calculations of several protein/ligand-docking scores. Xanthotoxin and angelicin were docked within the identified site with 100 possible conformations for each ranked according to the dock score provided in LigandFit. The binding conformation with the highest score and appropriate hydroxylation site closest to the heme was selected as the optimal conformation and subjected to energy minimization using the MMFF94 force field (Halgren 1996) in MOE while allowing full side chain relaxation. Heme coordinates were fixed to prevent distortion of the heme plane originating from bonded parameters in the MOE's implementation of the MMFF94 force field.

Results

Sequence Analyses and Phylogeny Construction

Five new allelic cDNA variants of the *CYP6B3* locus were cloned from *P. polyxenes* using the CYP6B3-specific primer set (GZF1/GZR1) spanning the length of the coding region. Three of the 5 variants with 99.4%–99.7% nucleotide identity encoded absolutely identical proteins and were designated CYP6B3v3a (DQ365694), v3b (DQ365695), and v3c (DQ365696); the 2 remaining variants were designated as CYP6B3v4 (DQ365697) and CYP6B3v5 (DQ365698). Compared with the previously cloned CYP6B3v1 (U25819) and CYP6B3v2 (U65488) (Hung et al. 1995, 1996), the most striking features of our newly cloned variants are the insertion of an A between position 464 and 465 and a deletion of C at position 471 of CYP6B3v1 and v2, resulting in a transient shift in the reading frame for 3 amino acids (positions 155 to 157). Pairwise comparisons of CYP6B3 variants, in terms of nucleotide and amino acid identities, with 3 CYP6B1 variants (CYP6B1v1 [M80828], CYP6B1v2 [M83117], and CYP6B1v3 [U05037]) from the

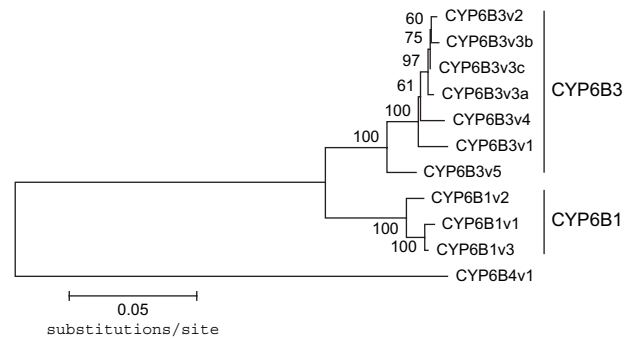
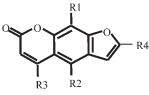
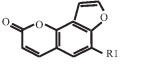
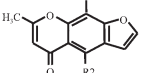
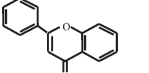
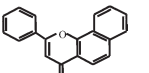
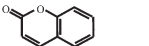


Fig. 1.—Phylogenetic relationship of CYP6B1 and CYP6B3 variants with CYP6B4 from *Papilio glaucus* as an outgroup. The neighbor-joining tree was constructed with p-distance of CDSs. The same topology was obtained with different methods including minimum evolution, maximum parsimony, and unweighted pair group method with arithmetic mean. The branch lengths are proportional to p-distances with numbers above the internal branches representing the bootstrap values calculated with 500 replications.

same species (Cohen et al. 1992; Prapaipong et al. 1994) and CYP6B4 (U47059) from *P. glaucus* (Hung et al. 1997) were presented in Supplementary Table 1 (Supplementary Material online). The phylogenetic relationship of CYP6B1 and CYP6B3 variants with CYP6B4 as an outgroup was constructed using neighbor-joining analysis (fig. 1). The topology of this phylogenetic tree was the same using different phylogenetic methods including minimum evolution, maximum parsimony, and unweighted pair group method with arithmetic mean.

Simple comparison of nucleotide and amino acid identities between sequences can sometimes be misleading in understanding the adaptive evolution of duplicated genes because differences at the nucleotide level do not necessarily translate to the differences at the amino acid level due to codon degeneracy. In addition, differences at the amino acid level do not necessarily translate into functional differences in protein structure and/or activity. This is especially the case for P450s where site-directed mutagenesis in several SRSs (Gotoh 1992) has shown these to be critical for function (Domanski and Halpert 2001). We therefore compared the substitution patterns of the CYP6B1 and CYP6B3 variants in their CDSs as well as in their SRS regions (table 1 and fig. 2) as previously defined for CYP6B1 and CYP6B8 (Sasabe et al. 2004). With an average of 13 SNPs per kb (p-distance of 0.013), CYP6B1 variants were comparable to the overall nucleotide heterogeneity detected in the nuclear genes of the mosquito *Aedes aegypti* (Morlais and Severson 2003). Specifically, the number of nucleotide substitutions in the CYP6B1 variants totaled 29 with 65.5% (19 out of 29) synonymous and 34.5% (10 out of 29) nonsynonymous. The 10 nonsynonymous substitutions translated into 9 amino acid replacements all occurring in non-SRS regions with 7 being highly conservative, 1 weakly conservative, and 1 nonconservative. Of the 4 nucleotide substitutions (13.8%) occurring in the SRS regions, all were synonymous and did not cause any amino acid replacements. The value of dS, the synonymous substitutions per site, was estimated to be 0.030 for the CDS which was much greater than the value of dN (0.007), the nonsynonymous substitutions per site. The ratio of dN/dS was 0.23. The difference between these 2

Table 2
Comparison of CYP6B1 and CYP6B3 Variant Activities toward Plant Allelochemicals

Structural Core	Chemicals	Structure				Activity (nmol/min/nmol Protein) \pm SE		
		R1	R2	R3	R4	CYP6B1v1	CYP6B3v3	CYP6B3v5
	Xanthotoxin	OCH ₃	H	H	H	25.1 (0.61) ^a	2.21 (0.27)	0.87 (0.11)
	Psoralen	H	H	H	H	16.9 (0.68) ^a	0.60 (0.05)	0.13 (0.02)
	Trioxsalen	CH ₃	H	CH ₃	CH ₃	7.6 (0.22)	2.86 (0.12)	0.85 (0.00)
	Isopimpinellin	OCH ₃	OCH ₃	H	H	19.6 (1.50)	2.47 (0.33)	0.50 (0.50)
	Angelicin	H				4.5 (0.14) ^a	0.74 (0.09)	0.38 (0.03)
	Sphondin	OCH ₃				3.0 (0.26)	1.00 (0.02)	0.33 (0.19)
	Visnagin	H	OCH ₃			0.36 (0.03) ^a	0.95 (0.08)	—
	Khellin	OCH ₃	OCH ₃			0.14 (0.04) ^a	1.99 (0.32)	—
	Flavone					0.56 (0.06) ^a	ND ^b	ND
	α -Naphthoflavone					0.56 (0.09) ^a	0.02 (0.01)	ND
	Coumarin					0.08 (0.05) ^a	ND	ND

^a Values were from Wen et al. 2005.

^b ND, not detected.

being highly conservative, 7 weakly conservative, and 9 nonconservative. Compared with the CYP6B1 variants, there were more substitutions in the SRS regions of the CYP6B3 proteins with a total of 15 substitutions (17.0%) of which 3 were nonsynonymous substitutions that included the conservative replacement of Leu108 in CYP6B3v1 with Ile108 in CYP6B3v3 and CYP6B3v5 occurring within the B' helix (SRS1), the conservative replacement of Gly369 in CYP6B3v1 and CYP6B3v3 with Ala369 in CYP6B3v5 occurring just downstream of the K helix (SRS5) and the conservative replacement of Ala485 in CYP6B3v1 and CYP6B3v3 with Val485 in CYP6B3v5 occurring in SRS6 near the C-terminus. Additional replacements among CYP6B3 variants also occurred in regions adjacent to these 6 defined SRS regions, specifically, the replacement of Thr289 in CYP6B3v1 with Ile289 in CYP6B3v3 and CYP6B3v5 occurred immediately upstream of the I helix (SRS4).

Activities of CYP6B1 and CYP6B3 Variants

With cDNAs of the new CYP6B3 variants already in the expression vector, we decided to express CYP6B3v3a and CYP6B3v5 for functional analyses because CYP6B3v3a encodes the same protein as CYP6B3v3b and CYP6B3v3c and is highly similar to CYP6B3v4 (99.2% amino acid identity) whereas CYP6B3v3 and CYP6B3v5 are more divergent (97.2% amino acid identity). Coexpression of the CYP6B3 variants as well as the previously characterized CYP6B1v1 variant in Sf9 cells with insect P450 reductase at MOI ratios determined to be nonlimiting for expression of this electron transfer partner indicated that, in most cases, these CYP6B3 variants metabolized substrates at rates lower than the CYP6B1v1 variant (table 2) except for furanochromones where CYP6B3v3 had higher rates. The

CYP6B1v1 variant displayed the highest activities toward linear furanocoumarins, substantially lower activities toward angular furanocoumarins and very low activities toward furanochromones, coumarin, and flavonoids. The CYP6B3 variants displayed no activity toward flavone and coumarin and marginal activity toward α -naphthoflavone.

With respect to the different linear furanocoumarins, CYP6B1v1 metabolizes methoxylated and unmodified furanocoumarins at higher efficiencies than trimethylated furanocoumarins and both CYP6B3v3 and CYP6B3v5 metabolize methoxylated and trimethylated furanocoumarins at higher efficiencies than unmodified furanocoumarins. Among the furanochromones tested, CYP6B3v3 metabolizes doubly methoxylated furanochromones at higher efficiency than singly methoxylated furanochromones whereas CYP6B1v1 has low activity toward both types.

To determine whether CYP6B1 and CYP6B3 variants metabolize xanthotoxin through the same pathway, [¹⁴C]-xanthotoxin was separately incubated with each of these enzymes coexpressed with P450 reductase, and the metabolites were TLC analyzed (fig. 3). Two major metabolites, M1 and M2, were detected for all enzymes in the presence of NADPH (lanes 5, 7, and 9). Second-phase addition of CYP6B3v3 or CYP6B3v5 with NADPH following first-phase metabolism of [¹⁴C] xanthotoxin with CYP6B1 and NADPH (lanes 10 and 11) generated the same 2 metabolites as reactions incubated only with CYP6B1 and NADPH (lane 5) indicating that CYP6B3 variants do not further metabolize the products of xanthotoxin metabolism by CYP6B1. Based on the conversion rate of [¹⁴C] xanthotoxin, this linear furanocoumarin is clearly metabolized by the 3 enzymes in the rank order of CYP6B1v1 \gg CYP6B3v3 > CYP6B3v5 that corresponds with the catalytic activities shown in table 2. Given that the [¹⁴C] xanthotoxin is labeled on its methoxy carbon, monooxygenation

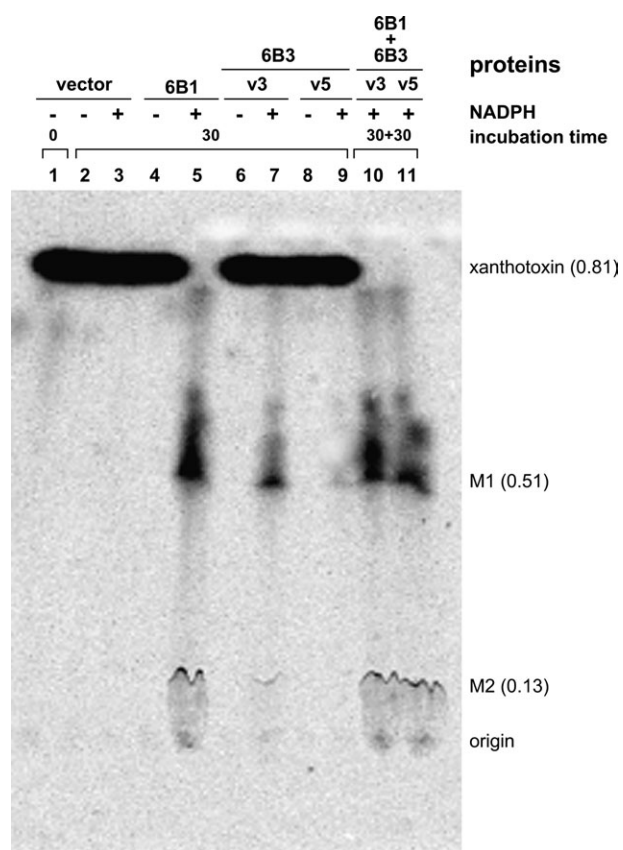


FIG. 3.—TLC analysis of [^{14}C]-labeled xanthotoxin metabolism by CYP6B1 and CYP6B3 variants. The reactions were incubated at 30°C in the absence (–) or presence (+) of NADPH. Individual enzymes (CYP6B1v1, CYP6B3v3a, or CYP6B3v5) were incubated for 30 min (lanes 1–9). Two phase incubations in the presence of NADPH were set up so that the first phase included only CYP6B1 and second phase included either CYP6B3v3a (lane 10) or CYP6B3v5 (lane 11). The 2 major metabolites of xanthotoxin were designated as M1 and M2 with their Rf values reported in parentheses.

does not occur on this position. The Rf values for xanthotoxin and the M1 and M2 metabolites were 0.89, 0.51, and 0.13 that are in the same relative distances as the Rf values obtained for xanthotoxin (0.67) and its 2 major structurally defined metabolites (0.46 and 0.12) in the midguts of *P. polyxenes* (Ivie et al. 1983). We have concluded that CYP6B1 and CYP6B3 metabolize xanthotoxin through the same detoxification mechanism to generate 2 major metabolites that are more water-soluble than the hydrophobic substrate.

Molecular Models of CYP6B3 Variants

To identify the positions of amino acid variations potentially contributing to these different catalytic efficiencies, molecular models for CYP6B1v1, CYP6B3v3, and CYP6B3v5 were constructed using alignments with 6 mammalian and 2 bacterial P450 sequences that are categorized as Class II P450s because they use P450 reductase as their electron transfer partner. With the alignment and modeling procedures with these 6 crystal structures detailed in Baudry et al. (2006), energy-minimized hybrid

Table 3
Predicted Interaction Energies and Distance between the Ferryl Oxygen in Heme and the Closest Hydrogen in the Furan Ring of Substrates (O-H Distance)

P450s	Substrates	Interaction Energy (kcal/mol)	O-H Distance (Å)
CYP6B1v1	Xanthotoxin	–33.6	2.7
	Angelicin	–27.5	2.4
CYP6B3v3	Xanthotoxin	–33.2	5.0
	Angelicin	–23.7	6.4
CYP6B3v5	Xanthotoxin	–29.9	5.9
	Angelicin	–26.4	7.7

models were built for CYP6B1v1, CYP6B3v3, and CYP6B3v5 using the CYP2A6 template (Yano et al. 2005) with replacement of the loop between strand 5 of β -sheet 1, B' helix, B helix, and B-C loop (collectively referred to as the B region that harbors SRS1) with that of the CYP2B4 template (Scott et al. 2004). This CYP6B1v1 model has slightly higher evaluation scores compared with the CYP6B1v1 model built using a single template alignment with bacterial CYP102 (Baudry et al. 2003). The best model for each protein was selected and further tested using Profiles 3D-1D analysis (Insight II Homology module, MSI, San Diego, CA) and Prosa II analysis (Center for Applied Molecular Engineering, University of Salzburg, Austria). Scores for the final models were as follows: Profiles 3D-1D for CYP6B1v1 (0.65), CYP6B3v3 (0.60), and CYP6B3v5 (0.6) and Prosa II for CYP6B1v1 (0.60), CYP6B3v3 (0.60), and CYP6B3v5 (0.60).

Each of these models was docked with representative linear (xanthotoxin) and angular (angelicin) furanocoumarins using LigandFit (Venkatachalam et al. 2003) implemented in the program Cerius2 (Version 4.10; Accelrys). For each substrate, 100 possible conformations were ranked according to the dock score provided in LigandFit and the binding conformation with the highest score and furan ring closest to the heme was selected as the optimal conformation and subjected to further energy minimization using the MMFF94 force field (Halgren 1996) in MOE. In the final substrate-docked CYP6B1v1 model, both xanthotoxin and angelicin are predicted to bind very close to the ferryl oxygen (2.7 Å and 2.4 Å, respectively) (table 3) and in a position nearly perpendicular to the heme plane (fig. 4). In the final CYP6B3 models, xanthotoxin and angelicin are predicted to bind substantially further away from the ferryl oxygen at distances of 5.0 Å and 6.4 Å for CYP6B3v3 and 5.9 Å and 7.7 Å for CYP6B3v5 (table 3) and in positions almost parallel to the heme plane.

The energy-minimized models built for the CYP6B3 variants indicate that the 14 amino acid differences between these proteins fall in the C-terminal region of the proteins with variations at some positions causing the CYP6B3v5 catalytic site to represent a hybrid between the CYP6B3v3 and CYP6B1v1 catalytic sites. Of the 6 catalytic site residues varying between CYP6B1v1 and CYP6B3v3 that are shown in figure 4, the first 4 (Ile108, Lys240, Tyr204, and Ala302) are identical between the 2 CYP6B3 variants and the remaining 2, Gly369 (SRS5) and Val485 (SRS6) in CYP6B3v3 are replaced by Ala369 and Ala485 in CYP6B3v5 and CYP6B1v1. Between the CYP6B3

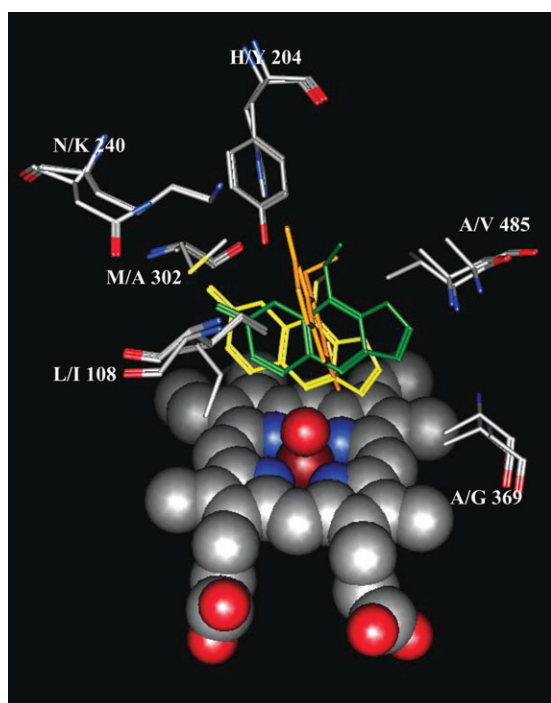


FIG. 4.—Predicted furanocoumarin binding modes in CYP6B1 and CYP6B3 models. The predicted binding orientation of xanthotoxin (orange for CYP6B1, yellow for CYP6B3v3, and green for CYP6B3v5) in the 3 energy-minimized models with the variable residues within 4 Å of xanthotoxin. In each pair, the first residue indicates that in CYP6B1 and the second indicates that in the CYP6B3v3 variant. At these positions, the CYP6B3v5 variant contains I108, K240, Y204, A302, A369, and A485.

variants, 3 additional changes occur in the β 1-3 strand and K' helix, another 2 in the K'' helix, 4 in the K helix and 3 occur in the β -sheet 4 region with all these variations falling outside the catalytic site. Comparison of these models indicates that the catalytic site of CYP6B3v3 contains many of the aromatic side chains previously identified as critical for maintaining the position of furanocoumarins in the catalytic site of CYP6B1v1 (Phe116, His117, Phe371, and Phe484) (Chen et al. 2002; Baudry et al. 2003; Pan et al. 2004). Conserved also are Ala113 and Ile115 that are important in defining substrate specificity and the rate of product exit from the CYP6B1v1 catalytic site (Pan et al. 2004; Wen et al. 2005). Interaction energies for the various binding modes are listed in table 3.

Discussion

In the ecological interactions between plant defense responses and herbivorous insects, attempts at counterdefense, duplication and subsequent functional divergence of genes involved in the synthesis of toxins by plants and the detoxification of toxins by insects have clearly played very important roles (Schuler 1996; Fogleman et al. 1998; Berenbaum 2002; Li et al. 2003; Feyereisen 2005; Ober 2005). In the study of the CYP6B proteins across *Papilio* species exposed to host plants with furanocoumarin levels ranging from low to high, Li et al. (2003) found that, following gene duplication, CYP6B proteins can evolve through time into more efficient and specialized

furanocoumarin-metabolizing CYP6B1-like proteins in *Papilio* species continuously exposed to furanocoumarins or less efficient enzymes as a result of relaxation of functional constraints in polyphagous species. In the current study, we have attempted to understand the evolution of 2 paralogous P450s, CYP6B1 and CYP6B3, from a species that is frequently exposed to furanocoumarins.

As a principal enzyme responsible for *P. polyxenes*' exclusive feeding on host plants containing toxic furanocoumarins, CYP6B1 was so important that several levels of constraints seemed to be in place to maintain its integrity. These include the facts that most nucleotide substitutions (65.5%) in the coding region are synonymous, only limited numbers of the substitutions (13.8%) occur in the SRS regions defining substrate specificity and are all synonymous and the 10 nonsynonymous substitutions (9 amino acid replacements) all occur in regions outside the catalytic site (non-SRS), and most (7 out of 9) are highly conservative. The value of dS, the synonymous substitutions per site, was estimated to be 0.030 for the CDS that was much greater than the value of dN (0.007), the nonsynonymous substitutions per site. The difference between these 2 parameters is further expanded in the SRS with dS being 0.034 and dN being 0.004. These results strongly suggest that CYP6B1 has been under intensive purifying selection following the duplication event that gave rise to CYP6B3.

CYP6B3, a paralog of CYP6B1 in *P. polyxenes*, has also been under purifying selection with somewhat relaxed selection constraints. Compared with CYP6B1, CYP6B3 had a higher degree of nucleotide heterogeneity with 18 SNPs in the coding region and 21 SNPs in the SRS regions. The nonsynonymous substitutions translated into 40 amino acid replacements with only 35% (14 out of 40) being conservative. CYP6B3 also had higher level of substitutions occurring in SRS (17%) with 3 being nonsynonymous. The ratios of dN/dS for the coding region and SRS were 0.25 and 0.19, respectively, for CYP6B3 in contrast to 0.23 and 0.12 for CYP6B1. These results strongly suggest that CYP6B3, though also under purifying selection following the duplication event, has evolved under much more relaxed constraints for both the coding region and SRS.

One model of gene evolution following duplication events is subfunctionalization where a pair of duplicate genes undergoes independent but complementary degenerative changes such that duplicates together retain the original functions of their single ancestor (Prince and Pickett 2002). The evolution of CYP6B1 and CYP6B3 has probably followed the subfunctionalization model. Consistent with our sequence analyses are the activities of the 2 enzymes that both metabolize xanthotoxin (a linear furanocoumarin) into the same 2 metabolites even though the metabolism of both linear and angular furanocoumarins by CYP6B1 is much more efficient compared with CYP6B3. Comparison of the molecular models derived for the CYP6B1v1, CYP6B3v3, and CYP6B3v5 docked with xanthotoxin and angelicin highlights the significant differences in the orientation of these 2 furanocoumarins and their distance from the heme iron and explains the differences in their catalytic activities.

The molecular models presented here predict that xanthotoxin and angelicin bind closer to the ferryl oxygen in

the CYP6B1v1 catalytic site than in either of the CYP6B3 variants as is consistent with the 10-fold higher activity of CYP6B1v1 with furanocoumarins and flavonoids. In addition, the highest ranking binding modes predicted for these substrates in the CYP6B1v1 model position the planar furanocoumarin molecule almost at a 90° angle to the heme plane whereas those predicted for the CYP6B3 variants position these substrates almost parallel to the heme plane. Close inspection of these models indicates that 3 greatest contributors to these position differences are: Leu108 (SRS1), His204 (SRS2), and Met302 (SRS4) in CYP6B1 versus Ile108, Tyr204, and Ala302 in the CYP6B3 variants as shown in figure 4. From these overlays, it appears that the large side chain of Met302 in CYP6B1 constricts the width of the catalytic site cavity in such a way that, with the smaller His204 at the top of the catalytic site, xanthotoxin and angelicin are able to position themselves upright and close to the ferryl oxygen. In this vertically oriented binding mode, His204 has potential to provide hydrogen bond acceptors/donors interacting with hydrogen bond donors/acceptors in the coumarin core of these furanocoumarins. In contrast, the smaller A302 in the CYP6B3 variants allows the substrates to rotate to a position parallel to the heme plane and moves the furan ring away from the reactive oxygen. Replacement of His204 and Leu108 with the bulkier Tyr204 and Ile108 further constricts the upper regions of the catalytic site. In this configuration, Tyr204 serves as a hydrogen bond donor stabilizing acceptor groups in the coumarin ring. Although close to the substrate, the effect of replacing Asn240 in CYP6B1v1 with Lys240 in the CYP6B3 alleles is not clarified by these comparisons but it is possible that the shorter side chain on asparagine provides more hydrogen bond acceptors/donors to the coumarin ring positioned in the upper regions of the CYP6B1 site whereas the longer lysine side chain performs this function in the CYP6B3 alleles because the coumarin rings of these substrates are located deeper in the active site cavity. These comparisons have also indicated that substrates bind in the CYP6B3v5 catalytic site even further away from the ferryl oxygen on heme. One residue that is the main contributor to this effect is Ala484 in CYP6B3v5 that opens the catalytic site cavity just above the furan ring; replacement of this with Val484 in CYP6B3v3 constricts the catalytic site and forces the furan ring to bind closer to the reactive oxygen.

The expression patterns of CYP6B1 and CYP6B3 are also in line with the subfunctionalization model where duplicated paralogs might involve a change in expression patterns (Hughes 2002). Whereas CYP6B1 transcripts were highly induced by xanthotoxin in midgut, fat body, and integument, CYP6B3 transcripts were more moderately induced by xanthotoxin only in fat body (Petersen et al. 2001). The expression patterns of these 2 P450s are also distinguished by the fact that CYP6B3 is induced by a wide range of linear and angular furanocoumarins including, in addition to xanthotoxin, bergapten, angelicin, and sphondin where CYP6B1 is induced by xanthotoxin and to a lesser extent by angelicin (Hung et al. 1995). That *P. polyxenes* maintains these 2 furanocoumarin-metabolizing loci with somewhat different activities and expression pattern provides it with the potential to evolve P450s with additional

functions, while it maintains those most critical to its exclusive feeding on current range of host plants. Coding region variations within these P450s may be important in evolving new functions for the many different types of allelochemicals encountered by this species.

Supplementary Material

Supplementary Table 1 is available at *Molecular Biology and Evolution* online (<http://www.mbe.oxfordjournals.org/>).

Acknowledgments

We thank Dr Arthur Zangerl for providing sphondin and insightful discussions and Dr Wenfu Mao for providing [¹⁴C] xanthotoxin. This work was funded by an Environmental Toxicology fellowship to G.N. and National Institutes of Health grant R01 GM071826 to M.A.S.

Literature Cited

- Baudry J, Li W, Pan L, Berenbaum MR, Schuler MA. 2003. Molecular docking of substrates and inhibitors in the catalytic site of CYP6B1, an insect cytochrome P450 monooxygenase. *Protein Eng.* 16:577–587.
- Baudry J, Rupasinghe S, Schuler MA. 2006. Class-dependent sequence alignment strategy improves the structural and functional modeling of P450s. *Protein Eng Des Sel.* 19:345–353.
- Berenbaum MR. 1991. Coumarins. In: Rosenthal G, Berenbaum M, editors. *Herbivores: their interactions with secondary plant metabolites*. Vol. 1. San Diego (CA): Academic Press. p. 221–249.
- Berenbaum MR. 2002. Postgenomic chemical ecology: from genetic code to ecological interactions. *J Chem Ecol.* 28:873–896.
- Bull DL, Ivie GW, Beier RC, Pryor NW. 1986. In vitro metabolism of a linear furanocoumarin (8-methoxypsoralen xanthotoxin) by mixed-function oxidases of larvae of black swallowtail butterfly and fall armyworm. *J Chem Ecol.* 12:885–892.
- Chen J-S, Berenbaum MR, Schuler MA. 2002. Amino acids in SRS1 and SRS6 are critical for furanocoumarin metabolism by CYP6B1v1, a cytochrome P450 monooxygenase. *Insect Mol Biol.* 11:175–186.
- Cohen MB, Schuler MA, Berenbaum MR. 1992. A host-inducible cytochrome P450 from a host-specific caterpillar: molecular cloning and evolution. *Proc Natl Acad Sci USA.* 89:10920–10924.
- Domanski TL, Halpert JR. 2001. Analysis of mammalian cytochrome P450 structure and function by site-directed mutagenesis. *Curr Drug Metab.* 2:117–137.
- Feyereisen R. 2005. Insect cytochrome P450. In: Gilbert LI, Iatrou K, Gill SS, editors. *Comprehensive molecular insect science*. Vol. 4. Oxford: Elsevier. p. 1–77.
- Fogleman JC, Danielson PB, MacIntyre RJ. 1998. The molecular basis of adaptation in *Drosophila*: the role of cytochrome P450s. *Evol Biol.* 30:15–77.
- Gonzalez FJ, Nebert DW. 1990. Evolution of the P450 gene superfamily. *Trends Genet.* 6:182–186.
- Gotoh O. 1992. Substrate recognition sites in cytochrome P450 family 2 (CYP2) proteins inferred from comparative analyses of amino acid and coding nucleotide sequences. *J Biol Chem.* 267:83–90.
- Halgren TA. 1996. Merck molecular force field. I. Basis, form, scope, parameterization, and performance of MMFF94. *J Comput Chem.* 17:490–519.
- Hughes AL. 2002. Adaptive evolution after gene duplication. *Trends Genet.* 18:433–434.

- Hung C-F, Berenbaum MR, Schuler MA. 1997. Isolation and characterization of CYP6B4, a furanocoumarin-inducible cytochrome P450 from a polyphagous caterpillar (Lepidoptera: papilionidae). *Insect Biochem Mol Biol.* 27:377–385.
- Hung C-F, Harrison TL, Berenbaum MR, Schuler MA. 1995. CYP6B3: a second furanocoumarin-inducible cytochrome P450 expressed in *Papilio polyxenes*. *Insect Mol Biol.* 4:149–160.
- Hung C-F, Holzmacher R, Connolly E, Berenbaum MR, Schuler MA. 1996. Conserved promoter elements in the *CYP6B* gene family suggest common ancestry for cytochrome P450 monooxygenases mediating furanocoumarin detoxification. *Proc Natl Acad Sci USA.* 93:12200–12205.
- Ivie GW, Bull DL, Beier RC, Pryor NW. 1987. Metabolic detoxification of linear and angular furanocoumarins by caterpillars of the black swallowtail butterfly—implications in host plant selection phenomena. In: Waller GR, editor. *Allelochemicals: role in agriculture and forestry*. (American Chemical Society Symposium Series 330). Washington (DC). p. 455–461.
- Ivie GW, Bull DL, Beier RC, Pryor NW, Oertli EH. 1983. Metabolic detoxification: mechanism of insect resistance to plant psoralens. *Science.* 221:374–376.
- Kumar S, Tamura K, Nei M. 2004. MEGA3: integrated software for molecular evolutionary genetics analysis and sequence alignment. *Brief Bioinform.* 5:150–163.
- Li W, Berenbaum MR, Schuler MA. 2001. Molecular analysis of multiple *CYP6B* genes from polyphagous *Papilio* species. *Insect Biochem Mol Biol.* 31:999–1011.
- Li W, Petersen RA, Schuler MA, Berenbaum MR. 2002. *CYP6B* cytochrome P450 monooxygenases from *Papilio canadensis* and *Papilio glaucus*; potential contributions of sequence divergence to host plant associations. *Insect Mol Biol.* 11:543–551.
- Li W, Schuler MA, Berenbaum MR. 2003. Diversification of furanocoumarin-metabolizing cytochrome P450s in two papilionids: specificity and substrate encounter rate. *Proc Natl Acad Sci USA.* 100:14593–14598.
- Long M, Betran E, Thornton K, Wang W. 2003. The origin of new genes: glimpses from the young and old. *Nat Rev Genet.* 4:865–875.
- Ma R, Cohen MB, Berenbaum MR, Schuler MA. 1994. Black swallowtail (*Papilio polyxenes*) alleles encode cytochrome P450s that selectively metabolize linear furanocoumarins. *Arch Biochem Biophys.* 310:332–340.
- Mao W, Rupasinghe S, Zangerl A, Schuler MA, Berenbaum MR. 2006. Remarkable substrate-specificity of CYP6AB3 in *Depressaria pastinacella*, a highly specialized caterpillar. *Insect Mol Biol.* 15:169–179.
- McDonnell CM, Brown RAP, Berenbaum MR, Schuler MA. 2004. Conserved regulatory elements in the promoters of 2 allelochemical-inducible cytochrome P450 genes differentially regulate transcription. *Insect Biochem Mol Biol.* 34:1129–1139.
- Meyer A, Van de Peer Y. 2003. ‘Natural selection merely modified while redundancy created’—Susumu Ohno’s idea of the evolutionary importance of gene and genome duplications. *J Struct Funct Genomics.* 3:vii–ix.
- Morlais I, Severson DW. 2003. Intraspecific DNA variation in nuclear genes of the mosquito *Aedes aegypti*. *Insect Mol Biol.* 12:631–639.
- Ober D. 2005. Seeing double: gene duplication and diversification in plant secondary metabolism. *Trends Plant Sci.* 10:444–449.
- Pan L, Wen Z, Baudry J, Berenbaum MR, Schuler MA. 2004. Identification of variable amino acids in the SRS1 region of CYP6B1 modulating furanocoumarin metabolism. *Arch Biochem Biophys.* 422:31–41.
- Petersen RA, Zangerl AR, Berenbaum MR, Schuler MA. 2001. Expression of *CYP6B1* and *CYP6B3* cytochrome P450 monooxygenases and furanocoumarin metabolism in different tissues of *Papilio polyxenes* (Lepidoptera: Papilionidae). *Insect Biochem Mol Biol.* 31:679–690.
- Prapaipong H, Berenbaum MR, Schuler MA. 1994. Transcriptional regulation of the *Papilio polyxenes CYP6B1* gene. *Nucleic Acids Res.* 22:3210–3217.
- Prince VE, Pickett FB. 2002. Splitting pairs: the diverging fates of duplicated genes. *Nat Rev Genet.* 3:827–837.
- Ravichandran KG, Boddupalli SS, Hasemann CA, Peterson JA, Deisenhofer J. 1993. Crystal structure of hemoprotein domain of P450BM-3, a prototype for microsomal P450s. *Science.* 261:731–736.
- Sasabe M, Wen Z, Berenbaum MR, Schuler MA. 2004. Molecular analysis of CYP321A1, a novel cytochrome P450 involved in metabolism of plant allelochemicals (furanocoumarins) and insecticides (cypermethrin) in *Helicoverpa zea*. *Gene.* 338:163–175.
- Schoch GA, Yano JK, Wester MR, Griffin KJ, Stout CD, Johnson EF. 2004. Structure of human microsomal cytochrome P450 2C8: evidence for a peripheral fatty acid binding site. *J Biol Chem.* 279:9497–9503.
- Schuler MA. 1996. The role of cytochrome P450 monooxygenases in plant-insect interactions. *Plant Physiol.* 112:1411–1419.
- Scott EE, White MA, He YA, Johnson EF, Stout CD, Halpert JR. 2004. Structure of mammalian cytochrome P450 2B4 complexed with 4-(4-chlorophenyl) imidazole at 1.9-Å resolution: insight into the range of P450 conformations and the coordination of redox partner binding. *J Biol Chem.* 279:27294–27301.
- Venkatachalam CM, Jiang X, Oldfield T, Waldman M. 2003. LigandFit: a novel method for the shape-directed rapid docking of ligands to protein active sites. *J Mol Graph Model.* 21:289–307.
- Wen Z, Baudry J, Berenbaum MR, Schuler MA. 2005. Ile115Leu mutation in the SRS1 region of an insect cytochrome P450 (CYP6B1) compromises substrate turnover via changes in a predicted product release channel. *Protein Eng Des Sel.* 18:191–199.
- Wen Z, Pan L, Berenbaum MR, Schuler MA. 2003. Metabolism of linear and angular furanocoumarins by *Papilio polyxenes* CYP6B1 coexpressed with NADPH cytochrome P450 reductase. *Insect Biochem Mol Biol.* 33:937–947.
- Wester MR, Johnson EF, Marques-Soares C, Dansette PM, Mansuy D, Stout CD. 2003. Structure of a substrate complex of mammalian cytochrome P450 2C5 at 2.3 Å resolution: evidence for multiple substrate binding modes. *Biochemistry.* 42:6370–6379.
- Williams PA, Cosme J, Ward A, Angove HC, Vinković DM, Jhoti H. 2003. Crystal structure of human cytochrome P450 2C9 with bound warfarin. *Nature.* 424:464–468.
- Yano JK, Blasco F, Li H, Schmid RD, Henne A, Poulos TL. 2003. Preliminary characterization and crystal structure of a thermostable cytochrome P450 from *Thermus thermophilus*. *J Biol Chem.* 278:608–616.
- Yano JK, Hsu MH, Griffin KJ, Stout CD, Johnson EF. 2005. Structures of human microsomal cytochrome P450 2A6 complexed with coumarin and methoxsalen. *Nat Struct Mol Biol.* 12:822–823.
- Yano JK, Wester MR, Schoch GA, Griffin KJ, Stout CD, Johnson EF. 2004. The structure of human microsomal cytochrome P450 3A4 determined by X-ray crystallography to 2.05-Å resolution. *J Biol Chem.* 279:38091–38094.
- Zhang J. 2003. Evolution by gene duplication: an update. *Trends Ecol Evol.* 18:292–298.

Adriana Briscoe, Associate Editor

Accepted September 7, 2006